ISBN: 978-3-95450-214-1 ISSN: 2673-5490 doi:10.18429/JACoW-IPAC2021-THPAB065

EXPERIMENTAL VERIFICATION OF THE SOURCE OF EXCESSIVE HELICAL SCU HEAT LOAD AT APS*

V. Sajaev, J. Dooling, K. Harkay, ANL, Argonne, IL, USA

Abstract

Immediately after the installation of the Helical Superconducting Undulator (HSCU) in the APS storage ring, higher than expected heating was observed in the cryogenic cooling system [1]. Steering the electron beam orbit in the upstream dipole reduced the amount of synchrotron radiation reaching into the HSCU and allowed the device to properly cool and operate. The simplest explanation of the excessive heat load was higher than expected heat transfer from the vacuum chamber to the magnet coils. However, modeling of the synchrotron radiation interaction with the HSCU vacuum chamber showed that Compton scattering could also result in synchrotron radiation penetrating the vacuum chamber and depositing energy directly into the HSCU coils [2]. In this paper we present experimental evidence that the excessive heat load of the HSCU coils is not caused by the heat transfer from the vacuum chamber but resulted from the synchrotron radiation penetrating the vacuum chamber.

INTRODUCTION

The HSCU cooling system was designed to handle the expected vacuum chamber heating, as confirmed by the test chamber measurements [3]. However, after injecting the first electron beam, unexpected heating of the magnet coils was observed, even though the vacuum chamber temperature was consistent with the predicted incident power. The magnet coil temperature exceeded 6 K when the stored beam current reached 80 mA (20% below the operational beam current of 100 mA). The HSCU cooling capacity was clearly exceeded because the LHe pressure was rising. The heating was the same for different beam fill patterns, which ruled out resistive wall or wakefield effects and pointed to synchrotron radiation. To reduce the synchrotron radiation heat load that was coming from the upstream bending magnet, the beam orbit was steered in the upstream dipole magnet to increase angle between the dipole exiting trajectory and HSCU axis. This causes the bigger part of the radiation from the end of the bending magnet to be intercepted upstream of the HSCU. Figure 1 shows the orbit bump that provides an additional 0.5 mrad orbit angle at the dipole exit. This orbit bump succeeded in reducing the temperature of the coils and allowed to turn on the magnet at full beam current.

EXPERIMENT

Synchrotron radiation can deposit power in the magnet coils in two ways. First, the synchrotron radiation directly strikes the vacuum chamber; the heat deposited in the chamber is then transferred to the magnet through thermal radiation or other thermal effects. Second, the synchrotron radiation may pass through the vacuum chamber (or scatter from it) and directly strike the magnet or magnet coils. The latter seems to be less likely since the incident angle of the radiation on the vacuum chamber is about 1.5 mrad, which results in a 1 m path length through the 1.5 mm-thick aluminum vacuum chamber.

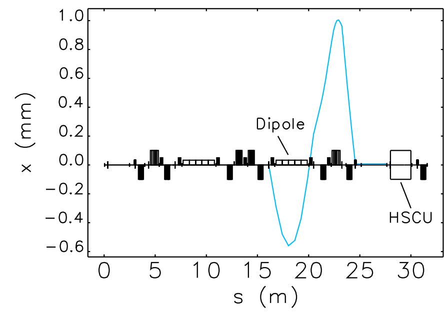

Figure 1: Orbit bump that generates positive orbit angle at the exit of the dipole, which only spans half the sector and has small overall orbit distortion. One lattice sector is shown.

To determine which magnet heating process dominates, an orbit bump amplitude scan was performed while recording the vacuum chamber and magnet coil temperatures. For each orbit bump, the dipole exit angle of the orbit changes, which means that the radiation that gets into the HSCU vacuum chamber is emitted from different parts of the dipole edge. It changes the total radiation power emitted into the HSCU chamber and also changes the spectrum of the radiation. The vacuum chamber temperature depends mostly on the total radiated power while the magnet temperature could also depend on the radiation spectrum, if the magnet heating is caused by the high-energy photons penetrating the vacuum chamber. To remove the effect of total power variation, the electron beam current was adjusted for every orbit bump to keep the vacuum chamber temperature approximately constant. Under these conditions, if the magnet heating is dominated by the heat transfer from the vacuum chamber, then the magnet temperature should also remain constant. On the other hand, if the magnet temperature changes while the vacuum chamber temperature stays constant, then the magnet heating is caused by radiation penetrating through the vacuum chamber.

The experiment was performed in March 2020 during beam studies. The wait time for the temperature settlement was chosen to be 20 minutes at each scan point. To determine the fully settled temperature, the time dependence of the temperature over the wait time was fitted with exponential decay:

$$T(t) = T_{\mathrm{eq}} + (T_0 - T_{\mathrm{eq}}) \exp\left({}^{-t}/_{\tau}\right),$$

* Work supported by the U.S. Department of Energy, Office of Science, Office of Basic Energy Sciences, under Contract No. DE-AC02-06CH11357.

ISBN: 978-3-95450-214-1 ISSN: 2673-5490 doi:10.18429/JACoW-IPAC2021-THPAB065

where T_0 and T_{eq} are the starting temperature and the temperature at equilibrium, and τ is the time constant of the process. The time constant of the vacuum chamber temperature settlement was found to be around 10 minutes while the time constant of the magnet was below 1 minute. Despite the long time constant for the vacuum chamber, since $(T_0 - T_{eq})/T_{eq}$ for the chamber was around 1–2% for all measurements, the 20 minutes wait time was still adequate. Figure 2 shows the typical temperature settlement process for both vacuum chamber and the magnet. The individual measurements on the plot are averaged over 7 neighboring points for better plotting results, while the exponential fits were performed using raw measurements.

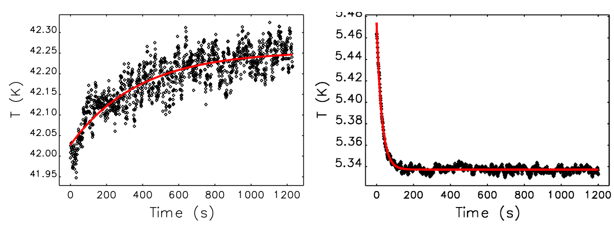

Figure 2: Typical temperature settlement during single scan point measurement. Left – vacuum chamber, right – magnet. Red line shows the exponential fit of the measured (black) points.

Figure 3 shows the results of the orbit bump scan. The top plot shows the vacuum chamber temperature as a function of the angle between the dipole-exiting trajectory and the HSCU axis. Only upstream and downstream temperatures are shown because the center sensor is broken. The plot also shows the electron beam current needed to minimize variations of the chamber temperature. The upstream and downstream parts of the chamber behave slightly differently, but in both cases the temperatures stay nearly constant, or increases slowly for the upstream sensor. The bottom plot shows temperatures of the upstream, center, and downstream parts of the magnet. One can see that while the vacuum chamber temperature does not change appreciably with bump amplitude, the magnet temperature actually goes down. This clearly shows that the magnet heating is not related to the vacuum chamber temperature, and therefore must be caused by something else — most plausibly, the radiation penetrating through the chamber.

SIMULATIONS

To understand how the synchrotron radiation power can get through the vacuum chamber, we first calculate the bending magnet field on the part of the trajectory from which the radiation is emitted into the HSCU vacuum chamber. APS bending magnets are 3-m-long and have a magnetic field of 0.6 T. The radiation that reaches into the HSCU vacuum chamber is emitted from the downstream edge of the magnet. Ray tracing and the measured dipole field map were used to find the magnetic field from which the radiation is emitted into the HSCU vacuum chamber. Figure 4 (left) shows the results of this calculation. One can see that the

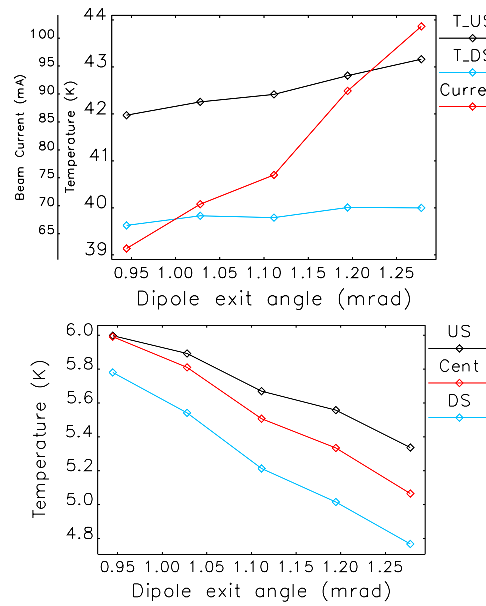

Figure 3: Vacuum chamber temperature (top) and magnet temperature (bottom) as a function of the dipole exit angle. Electron beam current is varied to keep the vacuum chamber temperature approximately constant (also shown on the top plot).

orbit bump lowers the maximum magnetic field from which the electron beam radiates into the HSCU chamber from about 0.5 T to 0.3 T, which in turn lowers the critical photon energy from 16 keV to 10 keV. The photon flux integrated over corresponding parts of trajectory is shown in Fig. 4 (right). One can see a sharp reduction of the number of high-energy photons when the orbit bump is applied. Using the fields shown in Fig. 4, the total power radiated into the chamber for 100 mA beam current was found to be 20 W without the bump and 10 W with the bump.

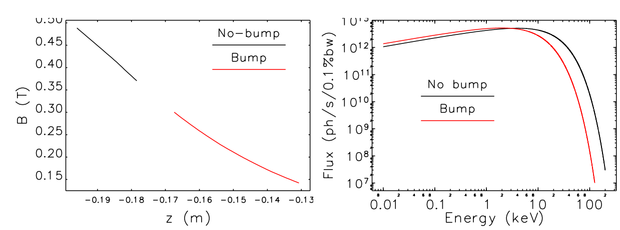

Figure 4: Left: Dipole field along the beam trajectory in the dipole showing only the regions radiating into the HSCU chamber. Right: Photon flux integrated over field regions shown on the left plot.

Analysis of photon interaction cross sections in the energy range of 10–100 keV shows the importance of Compton scattering in transferring synchrotron radiation power through the vacuum chamber into the magnet pole and coil region. Compton scattering becomes dominant in aluminum above 50 keV [4], where it can result in high-angle scattering events. For example, if a 60 keV photon loses 1 keV in a Compton scattering process, its angle will change by 31°. Therefore, even without large energy changes, Compton scattering can

ISBN: 978-3-95450-214-1 ISSN: 2673-5490 doi:10.18429/JACoW-IPAC2021-THPAB065

significantly reduce the path length of scattered photons through the vacuum chamber. This reduces the attenuation of the radiation and potentially leads to greater heating of the magnet and coils.

Simulations of photon scattering in the aluminum vacuum chamber were carried out using code MARS [5]. The MARS model uses a fairly accurate description of the HSCU vacuum chamber geometry [2]. A realistic spectral distribution for the synchrotron radiation photons was employed as input to MARS. To obtain reasonable statistics, a photon beam consisting of 10 million photons was used. It is important to note here that typical photon spectrum calculations are performed in units of photons per 0.1% of photon energy, while generating photons for MARS input requires to utilize the photon spectrum in units of photons per keV. Simulations showed significant streaming of photons through the chamber to the magnet region. Table 1 gives the deposited power for the vacuum chamber and magnet coils for the cases with and without the orbit bump. One can see that the orbit bump allowed reducing the power deposited in the magnet by about a factor of 10. For comparison, one can calculate the total radiated power above some photon energy using the photon flux shown in Fig. 4 (right). For example, there is 2.1 W above 40 keV for the case without orbit bump and 0.14 W for the case with orbit bump, which means that about one half of total energy above 40 keV penetrates the vacuum chamber.

Table 1: Deposited Power Due to Synchrotron Radiation Simulated by MARS for the Cases with and without Orbit Bump

	No Bump	**With Bump**
Vacuum chamber	19.4 W	10.6 W
Magnet	0.9 W	0.08 W
Total	20.3 W	10.7 W

Excess Cryocooler Capacity

The total beam-induced heat load on the magnet with the orbit bump in place can also be measured using the excess capacity of cryocoolers. The cryostat has a heater that is used to maintain the liquid helium tank pressure constant at 760 Torr. When the beam is injected in the ring, the heating of the magnet is increased due to beam-induced heat load. This results in reduction of the heater power required to keep the helium pressure constant, while the total power deposited into the cryostat remains constant.

In April 2020, the APS storage ring operated in a unique fill pattern – 324 bunches with top-up. This fill pattern provides the constant beam current without additional resistive wall losses associated with 24-bunch fill pattern. When the beam was injected into the ring after several hours-long break, the heater power required to keep the LHe tank pressure at 760 Torr reduced from 0.68 W to 0.58 W, as can be seen in Fig. 5. Reduction of the heater power by 0.1 W means that presence of the beam in the ring generated 0.1 W heat load on the 4 K circuit of the cryostat. Based on the measurements given in Table IV of [1], the expected heat transfer from the vacuum chamber to the magnet is 0.04 W. The inferred this way heat deposition in the magnet from the X-rays penetrating the chamber is 0.06 W, which compares favorably to the value of 0.08 W in Table 1.

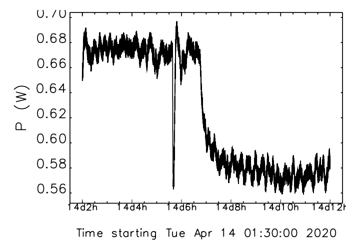

Figure 5: Reduction in heater power required to keep the LHe tank pressure at 760 Torr after the beam was injected into the ring.

CONCLUSIONS

We have performed an experiment where we clearly showed that the excessive heating of the HSCU magnet was caused by high-energy photons penetrating the aluminum vacuum chamber and not the increased heat transfer from vacuum chamber to the magnet. The experiment involved scanning orbit inside the upstream bending magnet to change the spectrum of the photons emitted into the HSCU vacuum chamber. At the same time we also varied the total beam current to keep the total power absorbed by the chamber the same. As result, we found that the magnet temperature was reducing with the orbit angle inside the bending magnet, while the vacuum chamber temperature stayed constant.

The effect of photons penetrating the vacuum chamber was not noticed in the previously installed SCUs for two reasons. First, due to their planar design, those devices do not have magnet coils in the horizontal plane, which is where the synchrotron radiation is concentrated. Second, the planar devices also allow for larger horizontal vacuum chamber gaps, which makes shielding of the chamber from the synchrotron radiation possible.

REFERENCES

[1] M. Kasa *et al.*, “Development and operating experience of a 1.2-m long helical superconducting undulator at the Argonne Advanced Photon Source”, *Phys. Rev. Accel. Beams*, vol. 23, p. 050701, 2020.
doi:10.1103/PhysRevAccelBeams.23.050701

[2] J. C. Dooling, R. J. Dejus, and V. Sajaev, “Synchrotron Radiation Heating of the Helical Superconducting Undulator”, in *Proc. 10th Int. Particle Accelerator Conf. (IPAC'19)*, Melbourne, Australia, May 2019, pp. 4328–4331.
doi:10.18429/JACoW-IPAC2019-THPTS093

[3] K. Harkay, private communication, Sep. 2017.

[4] XCOM, https://physics.nist.gov/PhysRefData/Xcom/Text/chap4.html

[5] N. V. Mokhov, “The MARS code system user's guide version 13(95)”, FNAL, Batavia, IL, USA, Rep. Fermilab-FN-628, 1995.